Acta Crystallographica Section F
Structural Biology and Crystallization Communications
ISSN 1744-3091

Crystallization and preliminary crystallographic studies of putative threonyl-tRNA synthetases from *Aeropyrum pernix* and *Sulfolobus tokodaii*

Satoru Shimizu,[a] Ella Czarina Magat Juan,[a]‡ Yu-ichiro Miyashita,[a] Yoshiteru Sato,[a]§ Md Mominul Hoque,[a] Kaoru Suzuki,[b] Masataka Yogiashi,[b] Masaru Tsunoda,[c] Anne-Catherine Dock-Bregeon,[d] Dino Moras,[d] Takeshi Sekiguchi[b] and Akio Takénaka[a,c]*

[a]Graduate School of Bioscience and Biotechnology, Tokyo Institute of Technology, Nagatsuda, Midori-ku, Yokohama 226-8501, Japan, [b]College of Science and Engineering, Iwaki-Meisei University, Chuodai-iino, Iwaki, Fukushima 970-8551, Japan, [c]Faculty of Pharmacy, Iwaki-Meisei University, Chuodai-iino, Iwaki, Fukushima 970-8551, Japan, and [d]Departement de Biologie et Génomique Structurales, Institut de Génétique et de Biologie Moléculaire et Cellulaire, 1 Rue Laurent Fries, F-67404 Illkirch, France

‡ Present address: Graduate School of Science, The University of Tokyo, 7-3-1- Hongo, Bunkyo-ku, Tokyo 113-0033, Japan.
§ Present address: Departement de Biologie et Génomique Structurales, Institut de Génétique et de Biologie Moléculaire et Cellulaire, 1 Rue Laurent Fries, F-67404 Illkirch, France.

Correspondence e-mail: atakenak@bio.titech.ac.jp, atakenak@iwakimu.ac.jp

Received 9 May 2008
Accepted 20 August 2008

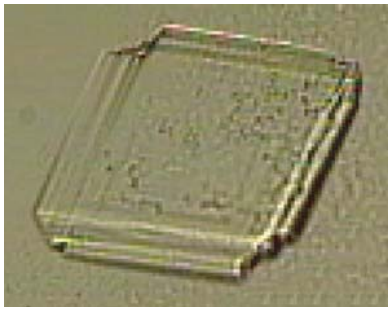

Threonyl-tRNA synthetase (ThrRS) plays an essential role in protein synthesis by catalyzing the aminoacylation of $tRNA^{Thr}$ and editing misacylation. ThrRS generally contains an N-terminal editing domain, a catalytic domain and an anticodon-binding domain. The sequences of the editing domain in ThrRSs from archaea differ from those in bacteria and eukaryotes. Furthermore, several creanarchaea including *Aeropyrum pernix* K1 and *Sulfolobus tokodaii* strain 7 contain two genes encoding either the catalytic or the editing domain of ThrRS. To reveal the structural basis for this evolutionary divergence, the two types of ThrRS from the crenarchaea *A. pernix* and *S. tokodaii* have been overexpressed in *Escherichia coli*, purified and crystallized by the hanging-drop vapour-diffusion method. Diffraction data were collected and the structure of a selenomethionine-labelled *A. pernix* type-1 ThrRS crystal has been solved using the MAD method.

1. Introduction

Aminoacyl-tRNA synthetases (aaRSs) play a crucial role in the biosynthesis of proteins by charging a cognate amino acid onto its cognate tRNA. This reaction takes place in two steps: (i) synthesis of an aminoacyladenylate intermediate by fusing ATP to the cognate amino acid and (ii) transfer of the amino-acid moiety to the 3′-terminus of the cognate tRNA to generate the aminoacyl-tRNA. In principle, aaRSs are not allowed to make any mistakes when catalyzing this two-step reaction. However, some aaRSs misactivate and misaminoacylate noncognate amino acids that are isosteric and chemically related to the cognate amino acids (Fersht & Kaethner, 1976; Igloi *et al.*, 1977; Schmidt & Schimmel, 1994). To maintain high fidelity of protein synthesis, these aaRSs usually translocate and hydrolyze the incorrect products at their editing domains[1].

A typical example is threonyl-tRNA synthetase (ThrRS), which generally consists of three domains: an N-terminal editing domain, a catalytic domain and a C-terminal anticodon-binding domain (Sankaranarayanan *et al.*, 1999; Torres-Larios *et al.*, 2003). This enzyme first synthesizes the threonyl-AMP intermediate and then transfers threonine onto $tRNA^{Thr}$. ThrRS must discriminate threonine from valine and serine. A conserved zinc ion in the catalytic domain precludes the misactivation of noncognate valine, resulting in the discrimination of valine (Sankaranarayanan *et al.*, 1999). In

[1] Two exceptions, known as nondiscriminating aaRSs, are aspartyl-tRNA synthetase (AspRS) and glutamyl-tRNA sunthetase (GluRS). The nondiscriminating AspRS (Sato *et al.*, 2007) produces Asp-$tRNA^{Asp}$ and Asp-$tRNA^{Asn}$ to compensate for the missing AsnRS. Similarly, GluRS produces Glu-$tRNA^{Glu}$ and Glu-$tRNA^{Gln}$ (Curnow *et al.*, 1997). The mischarged amino acids are amidated by other enzymes: GatCAB for Asp-$tRNA^{Asn}$ and GatED for Glu-$tRNA^{Gln}$.

Table 1
Protein purification and concentration procedures.

The columns used were from the following makers: Q-Sepharose Fast Flow, Superdex200, Resource ISO, Resource Q, HiLoad 16/60 Superdex75, HiLoad 16/60 Superdex200 and HiTrap Heparin HP were from Amersham Biosciences, Hydroxyapatite Type 1, BioScale CHT5I and Bioscale CHT10I were from Bio-Rad, Phenyl-Toyopearl Pak650S was from Tosoh and DEAE-celluose A500-sf from Seikagaku Biobusiness Corp. The concentrations, filter devices and buffers for the native and selenomethione-labelled protein pairs were identical. β-ME, β-mercaptoethanol.

Protein	*Ap*ThrRS-1	*Ap*ThrRS-2	*St*ThrRS-1	*St*ThrRS-2
Native				
First column	Q-Sepharose Fast Flow	Q-Sepharose Fast Flow	Resource ISO	Resource Q
Buffer *A*	50 m*M* potassium phosphate pH 7.0	50 m*M* potassium phosphate pH 7.0	20 m*M* Tris–HCl pH 8.0, 5 m*M* β-ME, 1.35 *M* $(NH_4)_2SO_4$	20 m*M* Tris–HCl pH 8.0, 5 m*M* β-ME, 50 m*M* NaCl
Buffer *B*	50 m*M* potassium phosphate pH 7.0, 200 m*M* NaCl	50 m*M* potassium phosphate pH 7.0, 500 m*M* NaCl	20 m*M* Tris–HCl pH 8.0, 5 m*M* β-ME	20 m*M* Tris–HCl pH 8.0, 5 m*M* β-ME, 600 m*M* NaCl
Second column	Hydroxyapatite Type 1	Phenyl-Toyopearl Pak650S	Resource Q	HiTrap Heparin HP
Buffer *A*	10 m*M* phosphate buffer pH 7.0	50 m*M* potassium phosphate pH 7.0	20 m*M* Tris–HCl pH 8.0, 5 m*M* β-ME	20 m*M* MES pH 6.0, 5 m*M* β-ME
Buffer *B*	250 m*M* phosphate buffer pH 7.0	50 m*M* potassium phosphate pH 7.0, 0.8 *M* $(NH_4)_2SO_4$	20 m*M* Tris–HCl pH 8.0, 5 m*M* β-ME, 2 *M* NaCl	20 m*M* MES pH 6.0, 5 m*M* β-ME, 700 m*M* NaCl
Third column	Superdex200	DEAE-celluose A500-sf	BioScale CHT5I	Bioscale CHT10I
Buffer *A*	50 m*M* potassium phosphate pH 7.0, 150 *M* NaCl	50 m*M* potassium phosphate pH 7.0	10 m*M* potassium phosphate pH 7.0, 5 m*M* β-ME	10 m*M* potassium phosphate pH 7.0, 5 m*M* β-ME
Buffer *B*	—	50 m*M* potassium phosphate pH 7.0, 500 m*M* NaCl	500 m*M* potassium phosphate pH 7.0, 5 m*M* β-ME	500 m*M* potassium phosphate pH 7.0, 5 m*M* β-ME
Fourth column	—	Superdex200	HiLoad 16/60 Superdex75	HiLoad 16/60 Superdex75
Buffer	—	50 m*M* potassium phosphate pH 7.0, 250 m*M* NaCl	20 m*M* Tris–HCl pH 8.0, 5 m*M* β-ME, 150 m*M* NaCl	20 m*M* Tris–HCl pH 8.0, 5 m*M* β-ME, 150 m*M* NaCl
Selenomethione derivative				
First column	Resource ISO		Resource ISO	Resource Q
Buffer *A*	20 m*M* Tris–HCl pH 8.0, 5 m*M* β-ME, 1.2 *M* $(NH_4)_2SO_4$		20 m*M* Tris–HCl pH 8.0, 5 m*M* β-ME, 1.5 *M* $(NH_4)_2SO_4$	20 m*M* Tris–HCl pH 8.0, 5 m*M* β-ME
Buffer *B*	20 m*M* Tris–HCl pH 8.0, 5 m*M* β-ME		20 m*M* Tris–HCl pH 8.0, 5 m*M* β-ME	20 m*M* Tris–HCl pH 8.0, 5 m*M* β-ME, 0.6 *M* NaCl
Second column	Resource Q		Resource Q	Bioscale CHT101
Buffer *A*	20 m*M* Tris–HCl pH 8.0, 5 m*M* β-ME		20 m*M* Tris–HCl pH 8.0, 5 m*M* β-ME	10 m*M* potassium phosphate pH 7.0, 5 m*M* β-ME
Buffer *B*	20 m*M* Tris–HCl pH 8.0, 5 m*M* β-ME, 0.6 *M* NaCl		20 m*M* Tris–HCl pH 8.0, 5 m*M* β-ME, 1 *M* NaCl	300 m*M* potassium phosphate pH 7.0, 5 m*M* β-ME
Third column	HiLoad 16/60 Superdex75		BioScale CHT5I	HiTrap Heparin HP
Buffer *A*	20 m*M* Tris–HCl pH 8.0, 5 m*M* β-ME, 150 m*M* NaCl		10 m*M* potassium phosphate pH 7.0, 5 m*M* β-ME	50 m*M* MES pH 6.0, 5 m*M* β-ME
Buffer *B*	—		500 m*M* potassium phosphate pH 7.0, 5 m*M* β-ME	50 m*M* MES pH 6.0, 5 m*M* β-ME, 0.6 *M* NaCl
Fourth column	—		HiLoad 16/60 Superdex75	HiLoad 16/60 Superdex75
Buffer	—		20 m*M* Tris–HCl pH 8.0, 5 m*M* β-ME, 150 m*M* NaCl	20 m*M* Tris–HCl pH 8.0, 5 m*M* β-ME, 150 m*M* NaCl
Concentration (mg ml^{-1})	6	5.8	5	3
Centrifugal filter†	Vivaspin 500	Microcon YM-10;	Centricon Ultracel YM-30	Centricon Ultracel YM-10
Buffer	20 m*M* potassium phosphate pH 7.0	20 m*M* potassium phosphate pH 7.0	20 m*M* Tris–HCl pH 7.0	20 m*M* HEPES pH 7.0

† The centrifugal filter devices were bought from the following: Vivaspin 500 from Sartorius Stedim Biotech, and Microcon and Centricon Ultracel from Millipore Co.

Escherichia coli, the N-terminal editing domain of ThrRS removes mischarged serine from Ser-tRNA^{Thr} (Dock-Bregeon *et al.*, 2004). However, the N-terminal domains of archaeal ThrRSs have no sequence homology to those of eukaryotic and bacterial ThrRSs. Nevertheless, it has been reported that the archaeal N-terminal domain is likewise able to remove serine mischarged onto tRNA^{Thr} (Beebe *et al.*, 2004). The structure of the N-terminal domain of *Pyrococcus abyssi* ThrRS (Hussain *et al.*, 2006) reveals similarities to that of D-aminoacyl-tRNA deacylase from *E. coli*, which specifically removes a D-amino acid mischarged on the tRNA.

Interestingly, several crenarchaeal species have been found to possess two different genes encoding ThrRSs (Woese *et al.*, 2000). Sequence alignments of these ThrRSs have shown that they diverge into two types, one resembling bacterial-type ThrRSs and the other containing archaeal-type sequences (Korencic *et al.*, 2004). In *Sulfolobus solfataricus*, the bacterial-type ThrRS possesses highly conserved catalytic and anticodon-binding domains, but has a large deletion in the N-terminal editing domain. This type of ThrRS, known as ThrRS-cat, can synthesize both Thr-tRNA^{Thr} and Ser-tRNA^{Thr} but does not discriminate against Ser-tRNA^{Thr}. In contrast, the archaeal-type ThrRS shows high conservation in the N-terminal editing domain but lacks the catalytic domain. This type of ThrRS, called ThrRS-ed, can hydrolyze misaminoacylated Ser-tRNA^{Thr} but does not have aminoacylation activity.

In the present study, further sequence analyses have been performed using the KEGG database (http://www.genome.jp/kegg/). Two other crenarchaeal organisms, *Aeropyrum pernix* (*Ap*) and *S. tokodaii* (*St*), each with two ThrRS genes of different origin (see §3.1 and Fig. 1) were identified. The sequences of the encoded ThrRSs are similar to those ThrRS-cat (*Ap*ThrRS-1 and *St*ThrRS-1) and ThrRS-ed (*Ap*ThrRS-2 and *St*ThrRS-2). In order to elucidate the structural basis of the editing and catalytic mechanisms in the two crenarchaea *A. pernix* and *S. tokodaii*, the two ThrRSs from both organisms were overexpressed in *E. coli* and purified. Crystals of the native and selenomethionine-labelled ThrRSs were obtained and X-ray diffraction data were collected. The structure of the selenomethionine-labelled *Ap*ThrRS-1 crystal has subsequently been solved using the Se-MAD method.

Table 2
Final crystallization conditions.

HEPES, 4-(2-hydroxyethyl)piperazine-1-ethanesulfonic acid titrated using NaOH; MES, 2-morpholinoethanesulfonic acid monohydrate titrated using NaOH; Tris–HCl, tris(hydroxymethyl)aminomethane titrated using HCl.

Crystal	*Ap*ThrRS-1	*Ap*ThrRS-2	*St*ThrRS-1	*St*ThrRS-2
Native				
Protein solution				
Buffer	20 m*M* potassium phosphate pH 7.0	20 m*M* potassium phosphate pH 7.0	20 m*M* Tris–HCl pH 7.0	20 m*M* HEPES pH 7.0
Concentration (mg ml^{-1})	6	5.8	5	3
Reservoir solution				
Buffer	0.1 *M* HEPES pH 7.5	0.1 *M* sodium acetate trihydrate pH 4.6	—	—
Precipitant	—	—	14% PEG 3350	12% PEG 3350
Salt	1.5 *M* ammonium sulfate	2.0 *M* sodium formate	0.3 *M* ammonium chloride	0.3 *M* ammonium sulfate
Growth time	One week	Six months	Two months	Two months
Selenomethionine derivative				
Protein solution				
Buffer	20 m*M* potassium phosphate pH 7.0		20 m*M* Tris pH 7.0	20 m*M* HEPES pH 7.0
Concentration (mg ml^{-1})	6		5	3
Reservoir solution				
Buffer	0.1 *M* HEPES pH 7.75		—	—
Precipitant	—		14% PEG 4000	10% PEG 3350
Salt	2.0 *M* ammonium sulfate		80 m*M* disodium hydrogen phosphate dihydrate	80 m*M* ammonium acetate
Growth time	One week	Six months	Two months	Two months

2. Materials and methods

2.1. Sequence comparison

The sequences of ThrRS-1 and ThrRS-2 from *A. pernix* (APE0809.1 and APE0117.1), from *S. tokodaii* (ST0966 and ST2187) and from other organisms in the *Sulfolobaceae* family (*S. solfataricus*, *S. acidocaldarius* and *Metallosphaera sedula*) were downloaded from the KEGG database. To analyze the structural modules, these sequences were compared with those of *E. coli* (*Ec*) and *P. abyssi* (*Pa*) ThrRSs using the program *ClustalX* (Thompson *et al.*, 1997).

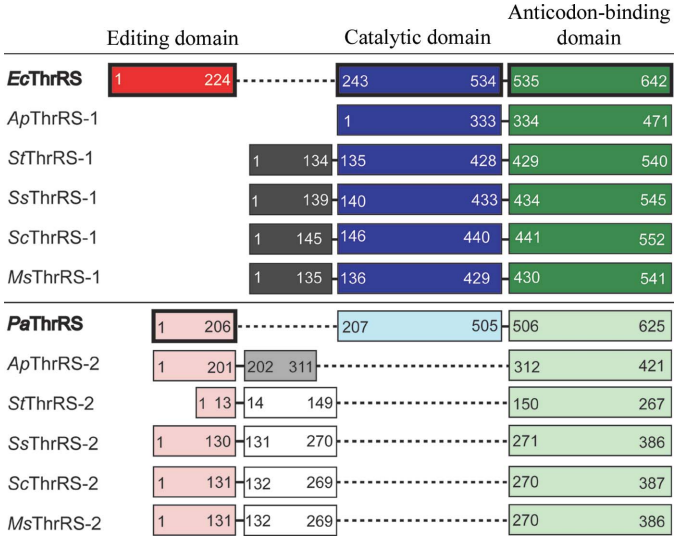

Figure 1
Schematic diagram showing the domain arrangement in various ThrRSs based on sequence alignments (see also supplementary material). Red and pink bars show the bacterial and archaeal editing domains, dark and light blue bars show the bacterial and archaeal catalytic domains and dark and light green bars show the bacterial and archaeal anticodon-binding domains, respectively. Bars of other colours are unknown regions. *Escherichia coli*, *Pyrococcus abyssi*, *Aeropyrum pernix*, *Sulfolobus tokodaii*, *S. solfataricus*, *S. acidocaldarius* and *Metallosphaera sedula* are abbreviated *Ec*, *Pa*, *Ap*, *St*, *Ss*, *Sa* and *Ms*, respectively. The thick-framed boxes indicate the domains for which three-dimensional structures have been obtained using X-ray crystallography (Sankaranarayanan *et al.*, 1999; Hussain *et al.*, 2006).

2.2. Overexpression and purification

The four genes encoding *Ap*ThrRS-1 (APE0809.1, 471 residues, 53 122 Da, pI 5.89), *Ap*ThrRS-2 (APE0117.1, 421 residues, 45 003 Da, pI 6.74), *St*ThrRS-1 (ST0966, 540 residues, 63 110 Da, pI 6.48) and *St*ThrRS-2 (ST2187, 267 residues, 30 855 Da, pI 6.93) were separately inserted into the pET11a vector (Novagen). The recombinant plasmids were introduced in *E. coli* Rosetta-gami (DE3) (Novagen) and the cells were grown in LB culture at 310 K. The selenomethionine derivatives were expressed in *E. coli* B834 (DE3) and BL21 (DE3) (Novagen) using minimal M9 medium containing L-selenomethionine. Following overnight incubation, the cells were harvested by centrifugation at 6000 rev min^{-1} for 10 min at 277 K and disrupted by sonication. The cell lysates were incubated at 343 K for 30 min to denature the *E. coli* proteins and centrifuged at 18 000 rev min^{-1} for 20 min at 277 K. The proteins were purified using the columns and

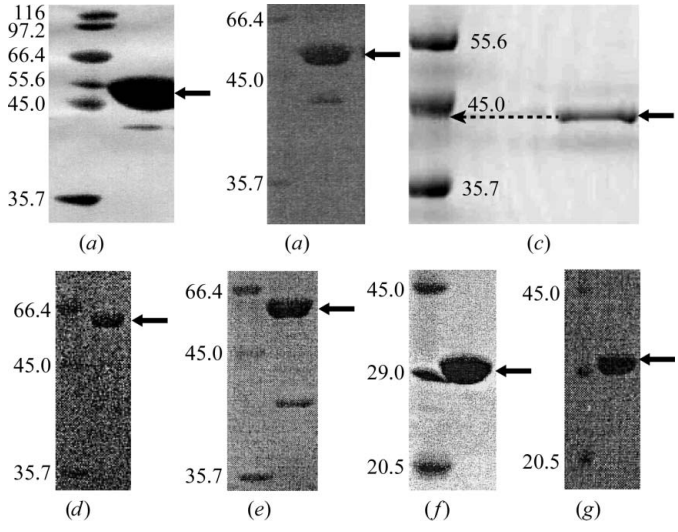

Figure 2
SDS–PAGEs of purified *Ap*ThrRS-1 (*a*) and its SeMet derivative (*b*), *Ap*ThrRS-2 (*c*), *St*ThrRS-1 (*d*) and its SeMet derivative (*e*) and *St*ThrRS-2 (*f*) and its SeMet derivative (*g*). Arrows indicate the purified sample bands; the adjacent columns contain molecular-weight markers (labelled in kDa).

Table 3
Data-collection and processing statistics for *Ap*ThrRS-1.

Values in parentheses are for the highest resolution shell.

		*Ap*ThrRS-1 (SeMet derivative)		
	*Ap*ThrRS-1	Peak	Edge	Remote
X-ray source	PF BL6A	PF BL17A		
Oscillation range (°)	1–180	1–360		
Wavelength (Å)	1.00	0.97898	0.97966	1.00
Space group	$C222_1$	$C222_1$		
Unit-cell parameters				
a (Å)	81.5	81.8	81.9	82.0
b (Å)	103.7	103.6	103.6	103.8
c (Å)	112.5	112.5	112.6	112.7
Z†	1			
Matthews coefficient (Å^3 Da^{-1})	2.2			
Solvent content (%)	45			
Resolution (Å)	50–2.3 (2.38–2.3)	50–2.5 (2.59–2.5)	50–2.5 (2.59–2.5)	50–2.5 (2.59–2.5)
Completeness (%)	100 (99.9)	100 (100)	100 (100)	100 (100)
$R_{\rm merge}$‡ (%)	9.6 (30.0)	8.3 (20.9)	8.4 (23.3)	8.0 (25.8)
Observed reflections	155186	244125	246544	240627
Unique reflections	21565	16854	17017	16636
Redundancy	7.2 (7.0)	14.5 (14.6)	14.5 (14.7)	14.5 (14.6)

† No. of subunits in the asymmetric unit. ‡ $R_{\rm merge} = 100 \times \sum_{hkl}\sum_i |I_i(hkl) - \langle I(hkl)\rangle| / \sum_{hkl}\sum_i I_i(hkl)$.

buffer solutions listed in Table 1. After purification, the proteins were concentrated to final concentrations of 3–15 mg ml^{-1} using centrifugal filter devices (Microcon and Centricon Ultracel YM-30 or YM-10 membrane from Millipore Co. or Vivaspin 500 from Sartorius Stedim Biotech; Table 1). The fractions obtained in all the purification steps as well as the concentrated proteins were analyzed by SDS–PAGE.

2.3. Crystallization

All crystallization trials were performed using the hanging-drop vapour-diffusion method by mixing equal volumes (1 µl) of the protein and reservoir solutions and equilibrating the mixed solutions against 700 µl reservoir solution in a 24-well plate at 293 K. Initial screening for potential crystallization conditions was performed using several kits purchased from Hampton Research Corporation (California, USA). The conditions under which crystalline precipitates appeared were optimized by changing the concentrations of the protein, precipitant and salt and by changing the pH of the buffer solution. The pH values and UV-absorption spectra were measured using an F-13 pH meter (Horiba Ltd, Japan) and a BioSpec-mini spectrophotometer (Shimadzu Corporation, Japan), respectively. For crystallizations, 24-well plates (Stem Corporation, Japan), plain glass cover slides (18 mm diameter Matsunami Glass Ind. Ltd, Japan) coated with silicon (L-25, Fuji Systems Corporation, Japan) and high-vacuum grease (Dow Corning Toray Co. Ltd, Japan) were used.

2.4. Data collection

The crystals obtained were soaked in their respective reservoir solutions containing 30% glycerol for 30 s and mounted on a CryoLoop (Hampton Research). X-ray diffraction measurements were performed at 95 K with 1° oscillation per image. Diffraction data were collected on the BL5A, BL6A, BL17A and NW12 beamlines of the Photon Factory (PF; Ibaraki, Japan) using a CCD detector (Area Detector Systems Co., ADSC, San Diego, California, USA). Diffraction images were indexed, integrated and scaled using the *HKL*-2000 package (Otwinowski & Minor, 1997) and intensity data were converted to amplitudes using programs from the *CCP*4 suite (Collaborative Computational Project, Number 4, 1994).

2.5. Preliminary structure analysis

The molecular-replacement and multiple anomalous dispersion (MAD) methods were applied to solve the phase problem. For molecular replacement, the programs *AMoRe* (Navaza, 1994), *MOLREP* (Vagin & Teplyakov, 2000) or *Phaser* (McCoy *et al.*, 2007) were employed and the ThrRS structures from *E. coli* (*Ec*ThrRS; PDB code 1qf6; Sankaranarayanan *et al.*, 1999, 2000) and *Staphylococcus aureus* (*Su*ThrRS; PDB code 1nyq; Torres-Larios *et al.*, 2003), truncated according to the sequence alignment, were used as search models. For MAD phasing, the programs *SHARP*/*autoSHARP* (Vonrhein *et al.*, 2007), *SHELXD* (Sheldrick, 2008), *SOLOMON* (Abrahams & Leslie, 1996) and *ARP*/*wARP* (Perrakis *et al.*, 1999) were used to calculate the phases, to locate heavy atoms, to modify the electron densities and to build the structures, respectively.

3. Results and discussion

3.1. Comparison of domain arrangement

Fig. 1 shows a schematic domain arrangement summarized from sequence comparisons between *Ec*ThrRS, *Pa*ThrRS, *Ap*ThrRS-1, *Ap*ThrRS-2, *St*ThrRS-1, *St*ThrRS-2, *Sf*ThrRS-1 (containing *Ss*ThrRS-1, *Sa*ThrRS-1 and *Ms*ThrRS-1) and *Sf*ThrRS-2 (containing *Ss*ThrRS-2, *Sa*ThrRS-2 and *Ms*ThrRS-2). More detailed diagrams are provided as supplementary material[2]. As pointed out by Korencic *et al.* (2004), *Ap*ThrRS-1 has a shorter sequence that only contains the residues of the catalytic and anticodon-binding domains. When compared with *Ec*ThrRS and *Pa*ThrRS, it is noteworthy that *St*ThrRS-1 and *Sf*ThrRS-1 have a short extension at the N-terminus of the catalytic domain. In contrast, crenarchaeal ThrRS-2s completely lack the catalytic domain. *Ap*ThrRS-2 and *Sf*ThrRS-2 have an editing domain similar to that of *Pa*ThrRS. In the case of *St*ThrRS-2, the corresponding editing domain displays high sequence conservation with *Pa*ThrRS, *Ap*ThrRS-2 and *Sf*ThrRS-2, but is much shorter at the N-terminus. In addition, crenarchaeal ThrRSs contain insertions

[2] Supplementary material has been deposited in the IUCr electronic archive (Reference: BO5044).

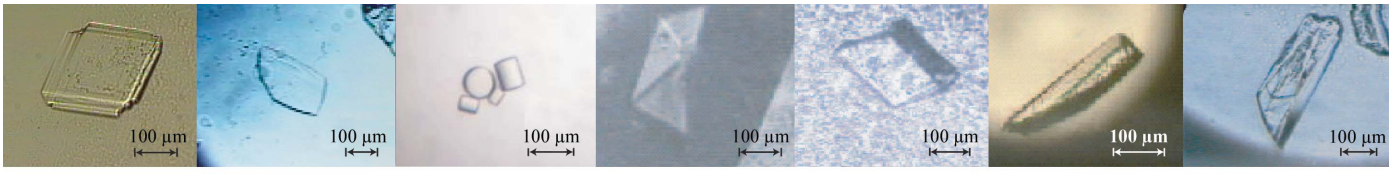

(*a*) (*b*) (*c*) (*d*) (*e*) (*f*) (*g*)

Figure 3
Crystals of *Ap*ThrRS-1 (*a*) and its SeMet derivative (*b*), *Ap*ThrRS-2 (*c*), *St*ThrRS-1 (*d*) and its SeMet derivative (*e*) and *St*ThrRS-2 (*f*) and its SeMet derivative (*g*). The crystallization conditions are described in Table 2.

Table 4
Data-collection and processing statistics for *St*ThrRS-1.

Values in parentheses are for the highest resolution shell.

		*St*ThrRS-1 (SeMet derivative)			
	*St*ThrRS-1	Peak	Edge	High remote	Low remote
X-ray source	PF-AR NW12	PF-AR NW12			
Oscillation range (°)	1–180	1–360			
Wavelength (Å)	1.00	0.97910	0.97942	0.96418	0.98030
Space group	$P2_1$	$P1$			
Unit-cell parameters					
a (Å)	68.8	71.1	70.9	70.9	70.9
b (Å)	99.7	85.7	85.5	85.5	85.6
c (Å)	85.3	104.1	103.9	103.8	104.0
α (°)	—	89.9	89.1	89.9	89.9
β (°)	95.0	92.3	92.3	92.3	92.3
γ (°)	—	95.4	95.2	95.2	95.2
Z†	2	2			
Matthews coefficient (Å^3 Da^{-1})	2.3	2.5			
Solvent content (%)	47	51			
Resolution (Å)	50–4.3 (4.45–4.3)	50–4.0 (4.14–4.0)	50–4.0 (4.14–4.0)	50–4.0 (4.14–4.0)	50–4.0 (4.14–4.0)
Completeness (%)	98.9 (98.1)	98.8 (98.1)	99.2 (99.2)	99.3 (99.2)	98.2 (99.2)
$R_{\rm merge}$‡ (%)	20.1 (31.1)	13.4 (32.7)	18.9 (50.0)	17.4 (47.1)	15.3 (38.4)
Observed reflections	27253	78967	79910	80233	75493
Unique reflections	7814	20429	20472	20559	20446
Redundancy	3.5 (3.5)	3.9 (3.9)	3.9 (3.9)	3.9 (3.9)	3.7 (3.4)

† No. of subunits in the asymmetric unit. ‡ $R_{\rm merge} = 100 \times \sum_{hkl} \sum_i |I_i(hkl) - \langle I(hkl)\rangle| / \sum_{hkl} \sum_i I_i(hkl)$.

Table 5
Data-collection and processing statistics for *St*ThrRS-2.

Values in parentheses are for the highest resolution shell.

		*St*ThrRS-2 (SeMet derivative)			
	*St*ThrRS-2	Peak	Edge	High remote	Low remote
X-ray source	PF BL5A	PF-AR NW12			
Oscillation range (°)	1–360	1–180			
Wavelength (Å)	1.00	0.97893	0.97907	0.96384	0.98295
Space group	$P2_12_12_1$	$P2_12_12_1$			
Unit-cell parameters					
a (Å)	60.3	60.5	60.5	60.5	60.6
b (Å)	68.0	67.9	67.8	67.9	67.9
c (Å)	134.4	134.2	133.9	133.8	134.0
Z†	2				
Matthews coefficient (Å^3 Da^{-1})	2.2				
Solvent content (%)	45				
Resolution (Å)	50–2.3 (2.38–2.3)	50–2.9 (3.0–2.9)	50–2.9 (3.0–2.9)	50–2.9 (3.0–2.9)	50–2.9 (3.0–2.9)
Completeness (%)	99.7 (100)	99.0 (100)	99.0 (100)	99.0 (100)	98.1 (99.9)
$R_{\rm merge}$‡ (%)	10.2 (30.3)	11.2 (26.7)	11.2 (26.7)	11.5 (29.0)	14.7 (36.4)
Observed reflections	328094	83055	83857	84524	73735
Unique reflections	25374	22735	22803	23010	22915
Redunduncy	12.9 (13.1)	3.7 (3.8)	3.7 (3.8)	3.7 (3.8)	3.3 (3.4)

† No. of subunits in the asymmetric unit. ‡ $R_{\rm merge} = 100 \times \sum_{hkl} \sum_i |I_i(hkl) - \langle I(hkl)\rangle| / \sum_{hkl} \sum_i I_i(hkl)$.

between the editing and anticodon-binding domains. X-ray analysis revealed that the *Pa*ThrRS editing domain forms a dimer (Hussain *et al.*, 2006). The interface of the dimer occurs between the shorter sequences commonly conserved in the editing domain of ThrRS-2s. Therefore, the editing domains of ThrRS-2s might form a dimer similar to that of *Pa*ThrRS.

3.2. Crystallizations

As shown in Fig. 2, every protein was highly purified prior to crystallization. Crystals of the native proteins and their SeMet derivatives (Fig. 3) were obtained under the conditions given in Table 2. In all cases, they do not contain ATP, amino acids or tRNA. The conditions for crystallization of the SeMet derivatives are similar to the corresponding conditions for native proteins, with the exception of SeMet *St*ThrRS-1, for which the reservoir solution added to the protein solution contained 80 m*M* Na_2HPO_4. Therefore, the difference in crystal habits between the *St*ThrRS-1 native and SeMet derivative crystals (described in §3.3) may be a consequence of the difference in their crystallization conditions. The conditions under which the *Ap*ThrRS-1 and *St*ThrRS-1 crystals were grown are similar, but differ from the reported conditions for *Ec*ThrRS (Sankaranarayanan *et al.*, 1999) and *Su*ThrRS (Torres-Larios *et al.*, 2002, 2003). Naturally, ThrRSs from different sources may crystallize under different conditions. Moreover, the conditions may vary between the present and previously reported ThrRS crystals because the latter were grown in complex with tRNA, ATP or a threonine analogue.

3.3. Data collection and structure determination

Fig. 4 shows examples of diffraction patterns obtained from the native crystals. The data-collection statistics for the *Ap*ThrRS-1, *St*ThrRS-1 and *St*ThrRS-2 crystals are summarized in Tables 3, 4 and 5, respectively. Although diffraction data were collected to 3.7 Å resolution from the *Ap*ThrRS-2 crystal, data-processing attempts were unsuccessful. The crystal data suggest that the native and

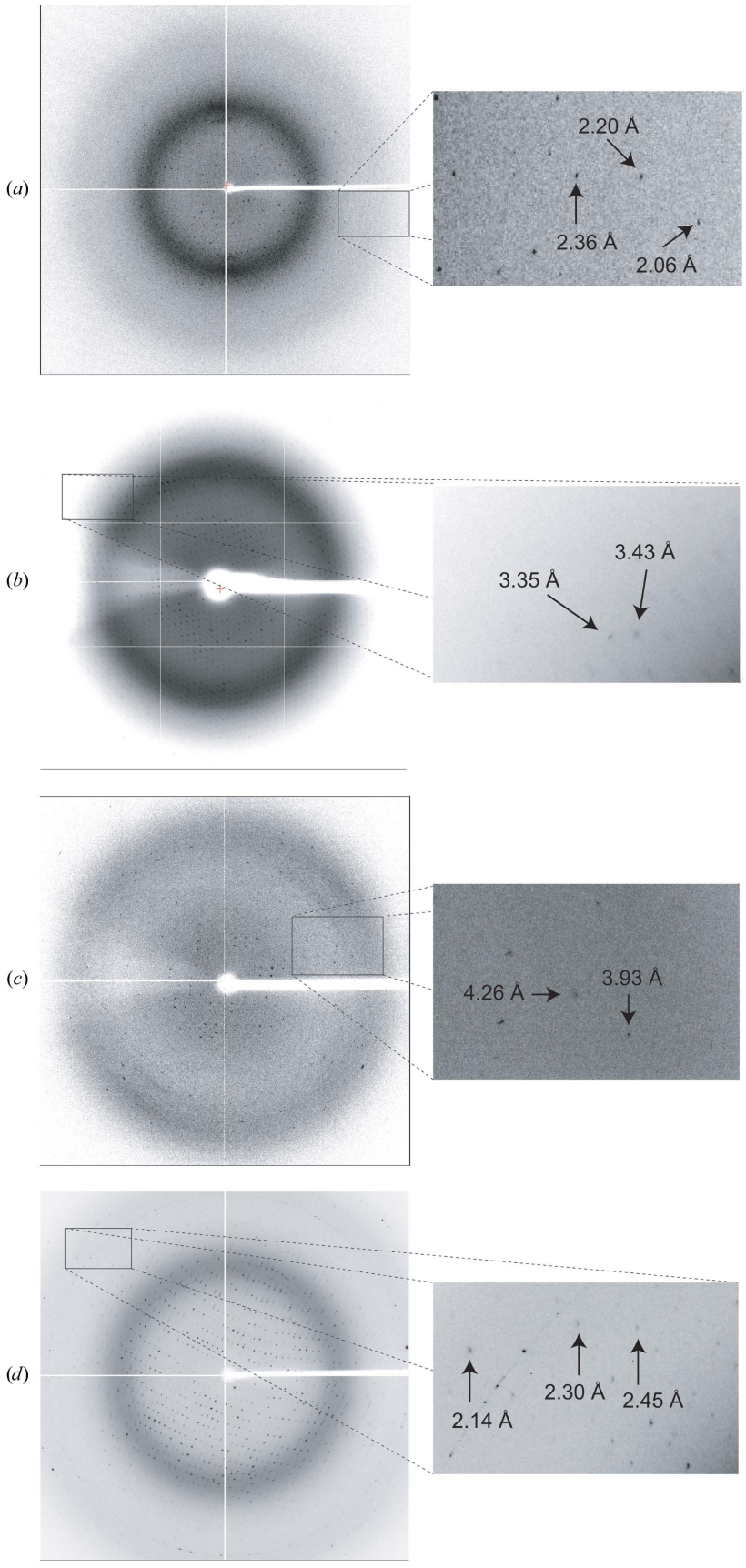

Figure 4
X-ray diffraction patterns of *Ap*ThrRS-1 (*a*), *Ap*ThrRS-2 (*b*), *St*ThrRS-1 (*c*) and *St*ThrRS-2 (*d*) crystals. The right column shows spots at the maximum resolution. Experimental conditions are described in Tables 3, 4 and 5.

selenomethionine-labelled pairs are isomorphous except for the *St*ThrRS-1 pair. The native and selenomethionine forms of *St*ThrRS-1 belong to space groups $P2_1$ and $P1$, respectively, and their unit-cell parameters differ. The calculated Matthews coefficients (Matthews, 1968) and the estimated solvent contents, which are also listed in Tables 3, 4 and 5, suggest that there is one subunit of *Ap*ThrRS-1 and two subunits of *St*ThrRS-1 or *St*ThrRS-2 in their respective asymmetric units. ThrRSs belong to the class II aaRSs (Eriani *et al.*, 1990; Cusack *et al.*, 1990), which generally form a homodimer through contacts between the catalytic domain of one subunit and the anti-codon-binding domain of another subunit. Therefore, in the case of the *Ap*ThrRS-1 crystal the two subunits must be related by crystallographic twofold symmetry in the $C222_1$ space group, even though the editing domain is missing.

Although several structures derived from ThrRS data published in the PDB were used as search models in molecular-replacement trials, it was difficult to obtain significant solutions. However, we have successfully completed phase determination for the selenomethionine derivative of *Ap*ThrRS-1 using the MAD method. 11 Se atoms with occupancies greater than 50% were found. After refinement of the atomic parameters, the electron-density map modified by the solvent-flattening technique shows a definite protein backbone, as shown in Fig. 5(*a*). The final correlation coefficient in $|E|^2$ was 0.771. After structure model building, more than 96% of protein residues were assigned. The statistics of structure modeling at the current stage are listed in Table 6. In parallel to refining the structure of *Ap*ThrRS-1, we are currently attempting to obtain crystals of higher quality for the selenomethionine-labelled *Ap*ThrRS-2, *St*ThrRS-1 and *St*ThrRS-2 proteins.

3.4. Preliminary structure of *Ap*ThrRS-1

As seen in Fig. 5(*b*), *Ap*ThrRS-1 forms a homodimer of subunits which are related to each other by crystallographic twofold rotation symmetry along the *a* axis. The amino-acid residues at the interface interact with each other through hydrogen bonds and van der Waals contacts between the two subunits. This structural feature is consistent with the dimer formation of the class II ThrRSs (Eriani *et al.*, 1990; Cusack *et al.*, 1990). The dimers are reasonably packed according to the space-group symmetry in the unit cell, with no molecular collisions, as seen in Fig. 5(*c*). More detailed structural features will be described elsewhere after full refinement.

3.5. Structural features of ThrRS-1 and ThrRS-2

The sequence comparison in Fig. 1 shows that the editing domain is completely missing in *Ap*ThrRS-1, while the other ThrRS-1s have additional small domains consisting of up to 145 amino-acid residues. In the ThrRS-2s, the editing domain of *Ap*ThrRS-2 is similar to that

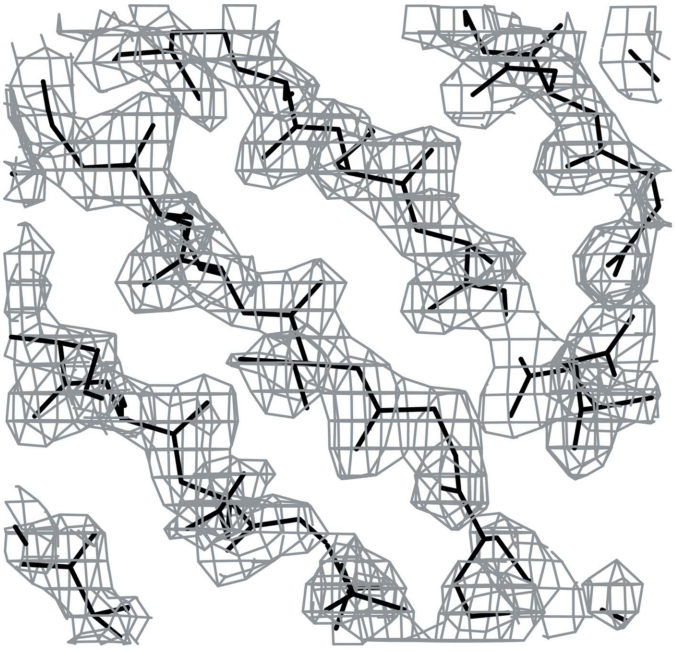

(*a*)

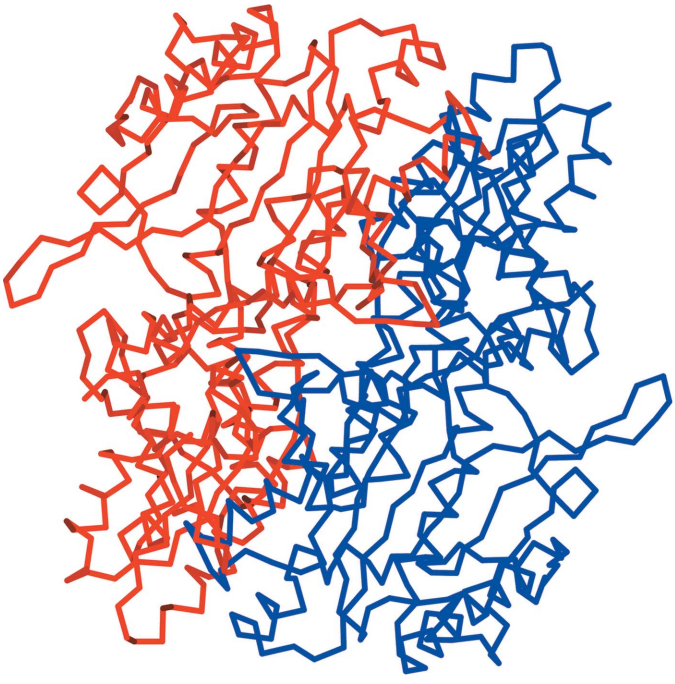

(*b*)

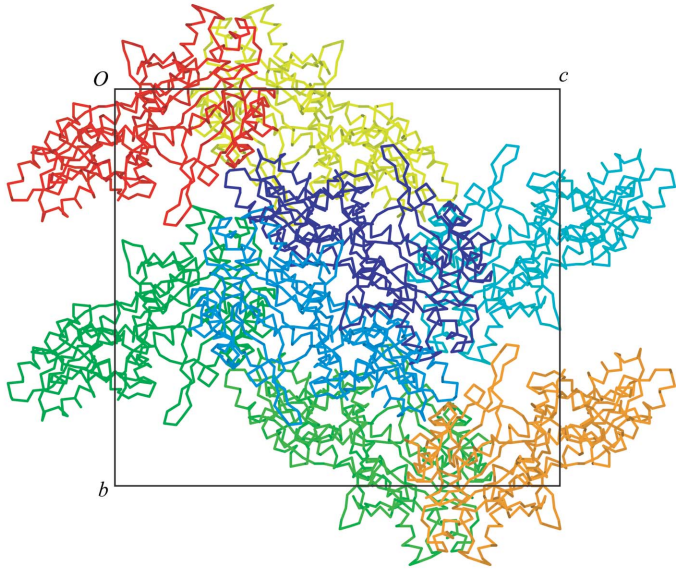

(*c*)

Figure 5
(*a*) $2|F_o| - |F_c|$ map (contoured at the 1.5σ level) of the *Ap*ThrRS-1 native crystal after structural model building with *ARP/wARP*, (*b*) the homodimer and (*c*) the molecular packing in the unit cell. The protein structures are drawn as C^α traces.

Table 6
Statistics of *Ap*ThrRS-1 structure modelling with *ARP*/*wARP*.

Resolution (Å)	50–2.3
R† (%)	21.2
R_{free}‡ (%)	28.5
Used reflections	20433
Assigned/total residues	451/471
Protein atoms	3626
Water molecules	258
Mean B value	15.26

† $R = 100 \times \sum \big||F_o| - |F_c|\big| / \sum |F_o|$, where $|F_o|$ and $|F_c|$ are the observed and calculated structure-factor amplitudes, respectively. ‡ Calculated using a random set containing 5% of observations that were not included throughout refinement (Brünger, 1992).

of *Pa*ThrRS. The domains of *Pa*ThrRS form a dimer similar to that of D-aminoacyl-tRNA deacylase from *E. coli* (Hussain *et al.*, 2006). Therefore, *Ap*ThrRS-2 might form a dimer between the editing domains, as the catalytic domain for dimerization is missing. This is consistent with the results of our gel-filtration experiment, which showed that the molecular size of *Ap*ThrRS-2 is equivalent to twice that of the subunit (data not shown). Here, it is interesting to note that the corresponding editing domain is extremely small in *St*ThrRS-2 but this part is just a dimerization interface to form a β-sheet between the two subunits. Furthermore, ThrRS-2 contains an additional domain just after the editing domain. This domain might be inserted to stabilize dimer formation, although the sequence of *Ap*ThrRS-2 is slightly different from the others. Both ThrRS-2 crystals contain two subunits in their asymmetric units, suggesting the possibility of dimer formation. These structural questions will be resolved by X-ray analyses of the four proteins *Ap*ThrRS-1, *Ap*ThrRS-2, *St*ThrRS-1 and *St*ThrRS-2.

This work was supported in part by Grants-in-Aid for the Protein3000 Research Program from the Ministry of Education, Culture, Sports, Science and Technology of Japan. We thank S. Kuramitsu for organizing the research group in the program and N. Igarashi and S. Wakatsuki for facilities and help during data collection.

References

Abrahams, J. P. & Leslie, A. G. W. (1996). *Acta Cryst.* D**52**, 30–42.
Beebe, K., Merriman, E., Ribas de Pouplana, L. & Schimmel, P. (2004). *Proc. Natl Acad. Sci. USA*, **101**, 5958–5963.
Brünger, A. T. (1992). *Nature (London)*, **355**, 472–475.
Collaborative Computational Project, Number 4 (1994). *Acta Cryst.* D**50**, 760–763.
Curnow, A. W., Hong, K., Yuan, R., Kim, S., Martins, O., Winkler, W., Henkin, T. M. & Söll, D. (1997). *Proc. Natl Acad. Sci. USA*, **94**, 11819–11826.
Cusack, S., Berthet-Colominas, C., Härtlein, M., Nassar, N. & Leberman, R. (1990). *Nature (London)*, **347**, 249–255.
Dock-Bregeon, A. C., Rees, B., Torres-Larios, A., Bey, G., Caillet, J. & Moras, D. (2004). *Mol. Cell*, **16**, 375–386.
Eriani, G., Delarue, M., Poch, O., Gangloff, J. & Moras, D. (1990). *Nature (London)*, **347**, 203–206.
Fersht, A. R. & Kaethner, M. M. (1976). *Biochemistry*, **15**, 3342–3346.
Hussain, T., Kruparani, S. P., Pal, B., Dock-Bregeon, A. C., Dwivedi, S., Shekar, M. R., Sureshbabu, K. & Sankaranarayanan, R. (2006). *EMBO J.* **25**, 4152–4162.
Igloi, G. L., von der Haar, F. & Cramer, F. (1977). *Biochemistry*, **16**, 1696–1702.
Korencic, D., Ahel, I., Schelert, J., Sacher, M., Ruan, B., Stathopoulos, C., Blum, P., Ibba, M. & Söll, D. (2004). *Proc. Natl Acad. Sci. USA*, **101**, 10260–10265.
Matthews, B. W. (1968). *J. Mol. Biol.* **33**, 491–497.
McCoy, A. J., Grosse-Kunstleve, R. W., Adams, P. D., Winn, M. D., Storoni, L. C. & Read, R. J. (2007). *J. Appl. Cryst.* **40**, 658–674.
Navaza, J. (1994). *Acta Cryst.* A**50**, 157–163.
Otwinowski, Z. & Minor, W. (1997). *Methods Enzymol.* **276**, 307–326.
Perrakis, A., Morris, R. M. & Lamzin, V. S. (1999). *Nature Struct. Biol.* **6**, 458–463.
Sankaranarayanan, R., Dock-Bregeon, A.-C., Rees, B., Bovee, M., Caillet, J., Romby, P., Francklyn, C. S. & Moras, D. (2000). *Nature Struct. Biol.* **7**, 461–465.
Sankaranarayanan, R., Dock-Bregeon, A.-C., Romby, P., Caillet, J., Springer, M., Rees, B., Ehresmann, C., Ehresmann, B. & Moras, D. (1999). *Cell*, **97**, 371–381.
Sato, Y., Maeda, Y., Shimizu, S., Hossain, M. T., Ubukata, S., Suzuki, K., Sekiguchi, T. & Takénaka, A. (2007). *Acta Cryst.* D**63**, 1042–1047.
Schmidt, E. & Schimmel, P. (1994). *Science*, **264**, 265–267.
Sheldrick, G. M. (2008). *Acta Cryst.* A**64**, 112–122.
Thompson, J. D., Gibson, T. J., Plewniak, F., Jeanmougin, F. & Higgins, D. G. (1997). *Nucleic Acids Res.* **25**, 4876–4882.
Torres-Larios, A., Dock-Bregeon, A.-C., Romby, P., Rees, B., Sankaranarayanan, R., Caillet, J., Springer, M., Ehresmann, C., Ehresmann, B. & Moras, D. (2002). *Nature Struct. Biol.* **9**, 343–347.
Torres-Larios, A., Sankaranarayanan, R., Rees, B., Dock-Bregeon, A.-C. & Moras, D. (2003). *J. Mol. Biol.* **331**, 201–211.
Vagin, A. & Teplyakov, A. (2000). *Acta Cryst.* D**56**, 1622–1624.
Vonrhein, C., Blanc, E., Roversi, P. & Bricogne, G. (2007). *Methods Mol. Biol.* **364**, 215–230.
Woese, C. R., Olsen, G. J., Ibba, M. & Söll, D. (2000). *Microbiol. Mol. Biol. Rev.* **64**, 202–236.